

## Pro-angiogenic and wound healing potential of baicalein: *In vitro*, *in ovo* and *in silico* evaluation

Krupa Ann Mathew<sup>1#</sup>, KM Bernadette<sup>1#</sup>, Annie John<sup>1,2</sup> & A Helen<sup>1\*</sup>

<sup>1</sup>Advanced Centre for Tissue Engineering (ACTE), Department of Biochemistry, University of Kerala, Thiruvananthapuram, Kerala, India

<sup>2</sup>Centre of Excellence in Stem Cell Research, Division of Biotechnology, Karunya Institute of Technology & Sciences, Coimbatore, Tamil Nadu, India

Received 31 January 2024; revised 31 March 2024

Angiogenesis is critical for the repair of damaged or diseased tissues. Hypoxia is a major factor promoting angiogenesis in physiological conditions. Baicalein, a flavone derived from the Chinese skullcap or Huangqin, *Scutellaria baicalensis* Georgi which is known to exhibit hypoxia mimetic activity. Here, we investigated the pro-angiogenic and wound healing potential of baicalein *in vitro*, *in ovo*, and *in silico* with a view to develop green wound dressings. The human keratinocyte cell line, HaCaT, was subjected to baicalein at varied concentrations *in vitro* and assessed for cell viability, cell cycle, and apoptosis induction. The study showed that lower concentrations of baicalein (below 10  $\mu$ M) promoted HaCaT proliferation, while higher concentrations induced apoptosis. Baicalein at low concentrations also promoted angiogenesis, as evidenced by the CAM (Chorioallantoic membrane) assay performed on chicken eggs. Gene expression analysis of Keratin 10 also suggested the activation of keratinocytes, leading to augmented wound healing after baicalein treatment. The *in silico* docking experiments reflect the potential of baicalein to promote angiogenesis via a HIF-independent pathway involving the agonistic transcriptional activation of the ERR $\alpha$ -PGC1 $\alpha$  complex. The results highlight the capability of baicalein to promote angiogenesis and wound healing and thus hold potential for the development of angiogenesis-promoting scaffolds and wound dressings.

**Keywords:** Angiogenesis, Chinese skullcap, Docking, Huangqin, Hypoxia, *Scutellaria baicalensis*

Cutaneous wound healing is a vastly dynamic and multifaceted process. Wound healing may broadly be divided into four phases: haemostasis, inflammation, proliferation and remodeling. It involves a multitude of different cell populations and chemical moieties that work in coordination. Cell-cell and cell-matrix interactions modulate cell proliferation, migration, and differentiation, which govern fibroplasia, epithelialization, and angiogenesis and lead to remodelling and wound contraction<sup>1</sup>.

Angiogenesis, characterized by the emergence of new vasculature from pre-existing vascular networks, is a normal biological process with a multitude of physiological implications. It facilitates the delivery of oxygen, nutrients, and biochemical cues, thereby aiding in the functional establishment of developing tissues. Angiogenesis is critical for repairing damaged or diseased tissues and occurs in the proliferative stage of wound healing. The main angiogenesis-

inducing factors are the vascular endothelial growth factor (VEGF), angiopoietin-1, angiopoietin-2, basic fibroblast growth factor (bFGF), and platelet-derived growth factor (PDGF)<sup>2</sup>. VEGF, the key mediator of angiogenesis, is primarily modulated via the hypoxia-induced stabilisation of the transcription factor, HIF-1 (hypoxia inducible factor-1)<sup>3</sup>, although HIF-1 independent pathways have also been implicated<sup>4,5</sup>. This pivotal role of angiogenesis in normal and pathological physiology is also suggestive of its central role in the successful integration of bioengineered constructs<sup>6</sup>. Incorporating angiogenesis-promoting components can overcome the challenge of efficient diffusion imposed by the dimensions of such bio-fabricated constructs.

Many therapeutics are designed to target and effect changes in pathways that belong to the distinct phases of wound healing. Baicalein, a flavone first isolated from the traditional medicinal plant Chinese skullcap or Huangqin (*Scutellaria baicalensis* Georgi), exhibits hypoxia mimetic, antioxidant, anti-inflammatory and antimicrobial activity<sup>7,8</sup>. Although baicalein is known to

\*Correspondence:

E-Mail: helenabiochem@gmail.com

#Contributed equally

exert many therapeutic effects<sup>8</sup>, most works focus on its anticancer properties<sup>9</sup>. There is still a dearth of information regarding its cutaneous wound healing properties and the mechanism of action. There are conflicting reports on the angiogenic effects of baicalein. While some authors report baicalein to be pro-angiogenic<sup>7,10-12</sup>, not much data is available in the context of wound healing. Conversely, there is also literature stating baicalein as being anti-angiogenic<sup>13,14</sup>. It may be presumed that similar to the apoptotic response observed in cancer cells<sup>9</sup>, the angiogenic response of baicalein is also dose-dependent. Alternatively, some authors propose the influence of cell type and disease microenvironment<sup>12</sup> as a potential explanation. But this ambiguity guarantees further exploration.

Efficient wound management is still a challenging clinical problem and emphasizes the need for efficient and new therapeutic strategies. When the healing of acute wounds does not progress in a timely order, it can progress to become a chronic wound. In this study, the wound healing and pro-angiogenic potential of baicalein was investigated *in vitro*, *in ovo* and *in silico*, with a view for developing green wound dressings and tissue-engineered constructs that would aid in skin regeneration. Since not much prior work is available on the impact of baicalein on cutaneous wound healing, *in vitro* and *in ovo* assessment would be more appropriate for a pilot study due to the cost-effectiveness and ease of performance. HaCaT, a human keratinocyte cell line extensively employed to investigate wound healing *in vitro*<sup>15</sup>, is used in the study. By virtue of its simplicity and similarity to *in vivo* physiology, *in ovo* systems are regularly used as model systems for studying angiogenic responses<sup>16</sup>. *In silico* experiments are economical options to get a focused viewpoint on the mode of action of baicalein before embarking into mechanistic studies. Overall, this study aims to ascertain how baicalein affects wound healing and angiogenesis in a dose-dependent manner and to delineate the underlying mechanisms.

## Materials and Methods

### Cell viability assay

HaCaT cells (human keratinocyte cell line) were maintained *in vitro* at 37°C in a humidified CO<sub>2</sub> (5%) incubator using DMEM (Dulbecco's Modified Eagle's Medium) (HiMedia, India) supplemented with 10% FBS<sup>15,17</sup>. Baicalein was purchased from Sigma-Aldrich, USA (Cat No: 465119; 98% purity). Baicalein was

dissolved in DMSO (Stock solution of 50 mM) and maintained at -80°C for long-term stable storage<sup>13</sup>. Due to its lower solubility, baicalein of the desired concentrations was prepared from the DMSO stock solution by dilution with either water or culture media. At a DMSO concentration of 0.1% and pH 7.4 of DMEM, the maximum solubility attainable was 200 µM. HaCaT cell line was treated with different concentrations of baicalein (0.1, 0.5, 1, 2.5, 5, 10, 25 and 50 µM) and cell viability was assessed by MTT assay (3-[4,5-dimethylthiazol-2-yl]-2,5 diphenyl tetrazolium bromide) after 24, 48 and 72 h of treatment. EZ Count MTT Cell Assay Kit (HiMedia, India) user manual and previous publications were referred for the protocol<sup>18</sup>. After incubation with MTT, the formazan crystals formed were dissolved in a solubilisation buffer, and absorbance was recorded at 570 nm.

### Cell cycle analysis

HaCaT cells cultured *in vitro* were treated with varied concentrations of baicalein (0.1, 2.5, 5, 10, 25, 50 and 100 µM) for 48 h, following which the cells were fixed on ice with 70% ethanol for 1 h. Washed cells were incubated with 1 mg/mL ribonuclease A (RNase A) (Sigma, USA) solution for 30 minutes and stained using 20 µg/mL propidium iodide (PI) (Sigma, USA) solution as per the protocol employed for HaCaT cells<sup>17</sup>. Cell cycle analysis was done using the flow cytometer by BD Biosciences (BD FACS Aria and BD FACS Diva software).

### Apoptosis detection by annexin V FITC- propidium iodide double staining

HaCaT cells were treated with baicalein (5 and 50 µM) for 48 h. Early and late stages of apoptosis were analysed by double staining using annexin V FITC-propidium iodide apoptosis detection kit (BD Pharmingen, USA) as per manufacturer's instructions. Cells were later examined by the FITC and PE (phycoerythrin) channels of the Flow cytometer (BD FACS Aria). As per literature, Betulinic acid (Merck, USA) at a concentration of 8 µg/ml for 48 hrs induced apoptosis in HaCaT cells and hence was used as the positive control for the experiment<sup>19,20</sup>.

### *In vitro* scratch wound assay

A wound was created on a monolayer of HaCaT cells using a sterile pipette tip and then subjected to treatment with baicalein at different concentrations (1, 2.5, 5, 10 and 50 µM) in low serum (1% FBS)<sup>21</sup>. Wound closure was imaged for up to 48 h, and the percentage of wound closure was estimated using ImageJ Software<sup>22</sup>.

### Gene expression analysis in HaCaT cells

HaCaT cells were grown to reach monolayer confluency and later subjected to scratch wound and treatment with 5  $\mu$ M of baicalein for 48 h. Cells were washed with PBS and harvested in the Trizol reagent, RNAiso Plus (Takara Bio, Japan). Chloroform-isopropanol method was used to isolate total RNA from the lysate. Total RNA was quantified and employed for subsequent cDNA synthesis using the Verso cDNA Synthesis Kit (Thermo Fisher Scientific, USA).

Quantitative Real-Time PCR (qPCR) analysis was done using QuantiNova SYBR Green PCR Kit (Qiagen, Germany) with CFX Opus Real-Time PCR Systems (Bio-Rad Laboratories, USA). The following conditions were preset for the PCR. The experiment was run sequentially at 95°C for 2 min, followed by 40 cycles of 95°C for 15 s, and later at 55°C for 10 s, and 68°C for 30 s. Relative gene expression was estimated by the comparative  $C_T$  ( $2^{-\Delta\Delta C_T}$ ) method from the  $C_q$  values obtained using the CFX Maestro Software (Bio-Rad Laboratories, USA). Beta actin was used to normalise the gene expression pattern. The primer sequences utilised for the qPCR are listed in Suppl. Table S1 [*All supplementary data are available only online along with the respective paper at the journal website (<http://ijeb.res.in>) as well as NOPR repository at <http://nopr.res.in>].*

### Chorioallantoic membrane (CAM) assay

Fertilised chicken eggs collected from the Regional Poultry Farm at Kudappanakunnu, Kerala, were surface sterilised and incubated at 37°C in humidified conditions. As per the previous literature<sup>16</sup>, about 3 mL of albumin was removed from the eggs using a 5 mL syringe on day 3. On day 4, filter discs (HiMedia, India) soaked with 20  $\mu$ L each of different concentrations of baicalein (1, 2.5, 5 and 10  $\mu$ M) were placed on the CAM in between the blood vessels through a window made on the eggshell. The windows were secured using surgical tapes, and the eggs were incubated for 72 h. After incubation, CAM was observed for the size and branching of the vessels. The captured images of CAM were analysed using ImageJ software.

### In silico docking analysis of baicalein

In order to elucidate the mechanism and pathways through which baicalein promotes angiogenesis, *in silico* analyses were performed. Both the HIF-dependent and independent pathways of angiogenesis were studied. Molecular docking was performed using the commercially licensed Maestro Molecular platform (Version 2021-1) by Schrödinger (Schrödinger,

LLC, New York) in NVIDIA DGX station A100 80 GB GPUs with server-grade CPU with Single AMD 7742, 128 cores, 2.25 GHz (base) –3.4 GHz (max boost) with 512 GB RAM running on Ubuntu Linux operating system 20.04.

Each protein 3-dimensional (3D) structure used for the docking experiment was downloaded from the Protein data bank (PDB) with specific PDB IDs. The PDB IDs of proteins employed in the docking analysis were 3OUJ, 1MZF, 2G1M, 1MZE and 7E2E. The PubChem ID of baicalein is 5281605. Each structure was refined, modified, and minimised as part of the protein preparation process, which was performed using the 'Protein Preparation Wizard' in the Schrödinger suite. The 'Prime' tool was used to locate and fill in any missing side chains, hydrogen atoms, or residues. It also corrects water molecules, heavy atoms, cofactors, and metal ions. The protein was subjected to energy minimisation utilising the OPLS4 force field to get the most stable energy state. A cubicle grid was created around the protein active region for grid creation to retain all functional amino acid residues attached (grid dimensions). The grid information of each PDB ID is listed in Suppl. Table S2.

The 'LigPrep' program was used to create the lowest energy 3D structures for the ligand optimisation using the OPLS4 force field. The ligand was prepared, tautomers were produced, and default settings were chosen. The 'GLIDE' ligand docking tool of Maestro was used for the molecular docking studies. The best-docked position and docking score were generated for each ligand.

## Results and Discussion

### Baicalein at lower concentrations promoted cell proliferation in HaCaT cells

Human keratinocyte cell line, HaCaT, cultured *in vitro*, were treated with baicalein at varied concentrations (0.1-50 $\mu$ M), and cell viability was assessed by MTT assay. Cell viability assay showed that baicalein exerts a proliferative effect on HaCaT cells (Fig. 1) at lower concentrations (0.1 – 10  $\mu$ M). A reduction in cell viability was identified at higher concentrations of baicalein (25 and 50  $\mu$ M).

The wound healing process is divided into an 'early phase,' characterised by the reestablishment of homeostasis, and a 'cellular phase,' ultimately restoring the wounded tissue<sup>1</sup>. The 'cellular phase' consists of cascades of overlapping and parallel events, mainly inflammatory, proliferative, and remodeling phases. The proliferative phase of wound healing unfolds with the

migration to and the proliferation of fibroblasts at the wound area (fibroplasia). It proceeds with the generation of the granulation tissue, a make-shift extracellular matrix (ECM) consisting of the ground substances (e.g.,

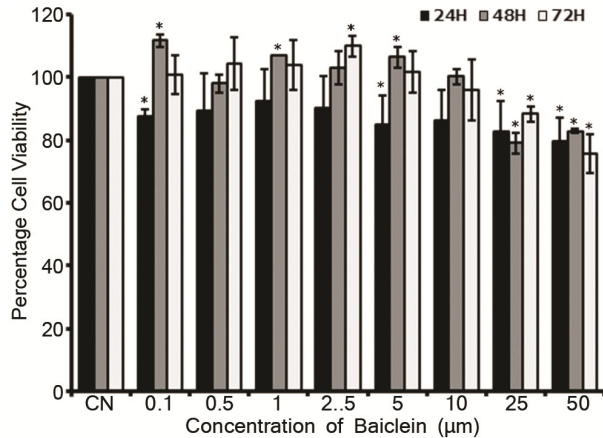


Fig. 1 — Cell viability assessment by MTT assay. Bar graph showing mean  $\pm$  SD values of percentage cell viability of HaCaT cells after 24, 48 and 72 h of treatment with baicalein ranging from 0.1 – 50  $\mu$ M (n=3). [*\*P* < 0.05 compared to control of each time]

fibronectin and collagen) secreted by the fibroblasts. Granulation tissue aids in the migration and adhesion of fibroblasts, endothelial cells, and epithelial cells on the wound bed, leading to fibroplasia, angiogenesis, and reepithelialisation during wound healing. Basal keratinocytes, the key cell type involved in the reepithelialisation phase of wound healing, migrate, proliferate, and differentiate over the wound bed, thereby reinstating the epithelial layer of the wounded skin<sup>23, 24</sup>. Hence, the observed proliferative potential of baicalein on the human keratinocyte cell line HaCaT, as evidenced in the cell viability assay, is indicative of its wound healing potential.

**Higher concentrations of baicalein initiated apoptosis in HaCaT cells**

The ethanol-fixed HaCaT cells, after incubating with RNase A and staining with PI, generated a typical cell cycle histogram when analysed with a flow cytometer (Fig. 2). The cell population could be delineated into Sub G<sub>0</sub>, G<sub>0</sub>/G<sub>1</sub>, S, and G<sub>2</sub>/M cell cycle stages by gating. It was observed that during baicalein treatment, the

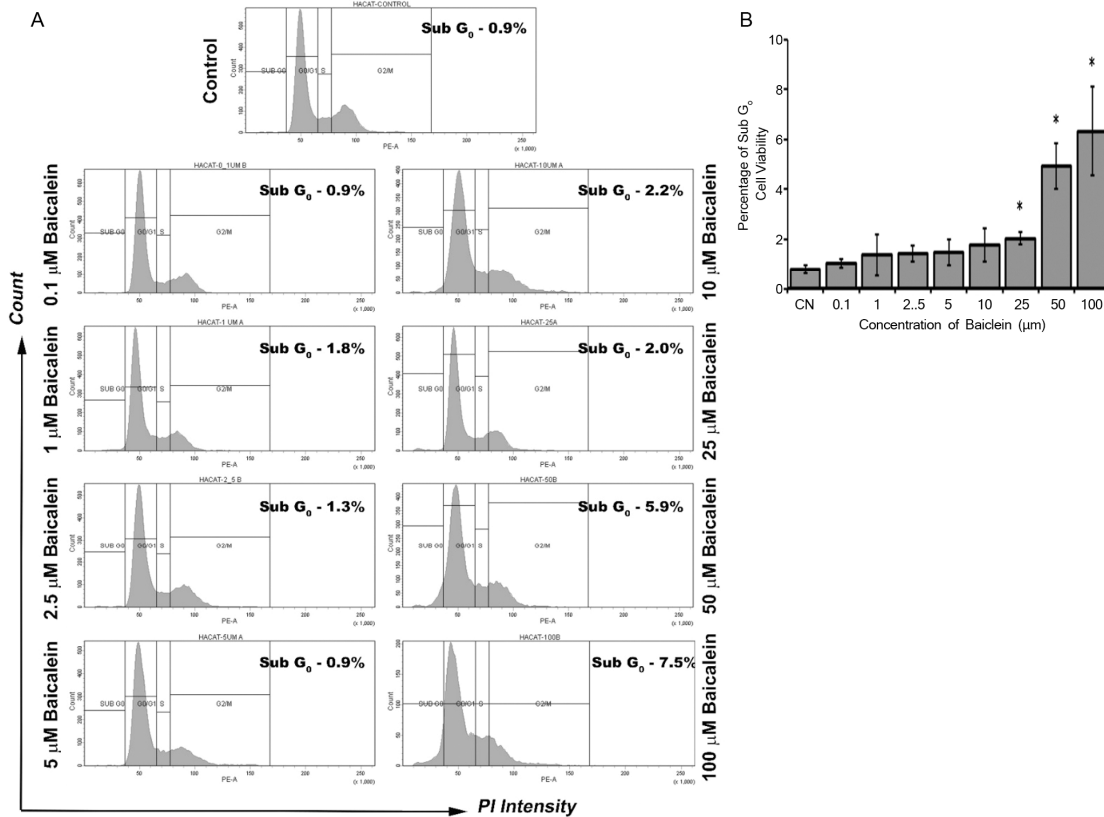


Fig. 2 — Cell cycle analysis. (A) Following 48 h of treatment of HaCaT cells with different concentrations of baicalein and subsequent PI staining, histograms (PI intensity against Cell count) were generated through flow cytometry. Each histogram is gated into four regions representing cell populations in different cell cycle stages: Sub G<sub>0</sub>, G<sub>0</sub>/G<sub>1</sub>, S and G<sub>2</sub>/M. The percentage cell population in the Sub G<sub>0</sub> phase corresponding to each sample is mentioned in the histogram. (B) Bar graph showing the percentage cell population (mean  $\pm$  SD) in Sub G<sub>0</sub> phase of the cell cycle after baicalein treatment.(n=3) [*\*P* < 0.05, compared to control]

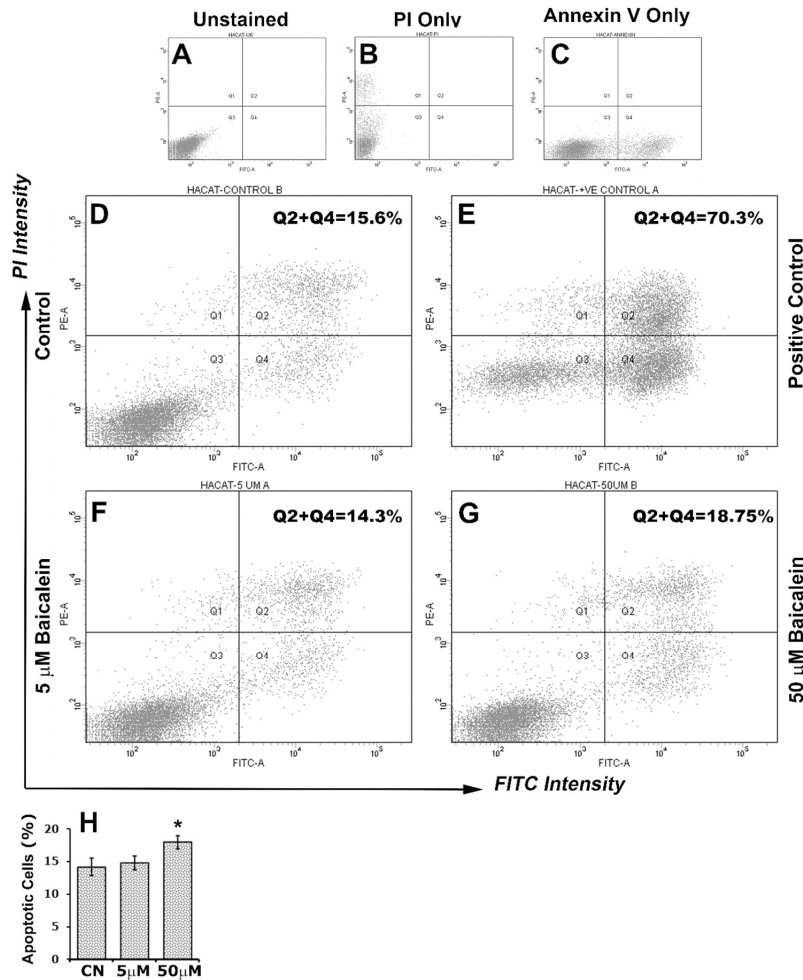


Fig. 3 — Representative dot plots (FITC Intensity vs. PI Intensity) of flow cytometric detection of cell death by annexin V-PI method in HaCaT cells treated for 48 h with (D) medium alone control, (E) betulinic acid positive control, (F) 5  $\mu$ M and (F) 50  $\mu$ M of baicalein. Plots A, B and C represent the patterns obtained when control cells were unstained, stained with PI alone and stained with FITC-Annexin V alone, respectively. The plot area is divided into four quadrants, namely, Q1, Q2, Q3 and Q4. The total percentage of cell population in both Q2 and Q4 for each sample is mentioned in the corresponding dot plots. (H) Graphical representation of the average percentage of apoptotic cells (Q2+Q4) from three experiments after indicated baicalein treatments. [ $*P < 0.05$ , compared to control]

percentage of cells lodging the Sub  $G_0$  phase of the cell cycle increased with an increase in the concentration of baicalein. The average percentage of cells in the Sub  $G_0$  phase after treatment with 100  $\mu$ M of baicalein was 6.3 compared to 0.8 in the case of control cells. This result is indicative of the apoptosis-inducing potential of higher concentrations of baicalein.

In order to study the pro-apoptotic potential of higher concentrations of baicalein, an apoptosis detection assay was done by double staining with annexin V FITC- Propidium Iodide. Cells, during the early stages of apoptosis, lose their plasma membrane integrity, characterised by the externalisation of phosphatidylserine (PS) phospholipid from the inner surface to the outer surface of the plasma membrane.

Annexin V is a phospholipid-binding protein specific to the exposed PS. Hence, FITC conjugated annexin V positivity is suggestive of earlier stages of apoptosis. PI is a DNA-binding dye that can readily stain dead cells with damaged membranes more readily than live cells with undamaged membranes. Hence, dual staining with annexin V and PI can differentiate between early and late apoptosis cells. Early apoptotic cells will be FITC-Annexin V positive but PI negative. Meanwhile, late apoptotic cells will be positive for both FITC-Annexin V and PI.

The dot plots generated by the FACS Diva software were divided into four quadrants, namely, Q1, Q2, Q3 and Q4 (Fig. 3). The Q2 quadrant (right-upper) represents the late apoptotic population, while

the Q4 quadrant (right-lower) represents the early apoptotic population. Both Q2 and Q4 represent the total apoptotic population (Q2+Q4). The unstained sample showed no signals in the Q2 and Q4 quadrants (Fig. 3A). An increased apoptotic population (70.3%) was obtained in positive control, confirming the accuracy of the protocol and quadrant-gating (Fig. 3E). Treatment with a higher concentration of baicalein (50  $\mu\text{M}$ ) for 48 h increased the percentage of apoptotic cell population in HaCaT cells (Fig. 3G) than treatment with a lower concentration of baicalein (5  $\mu\text{M}$ ) (Fig. 3F) and untreated control (Fig. 3D).

Hence, it can be concluded from MTT assay, cell cycle analysis, and apoptosis detection assay that lower concentrations of baicalein (below 10  $\mu\text{M}$ ) were nontoxic to HaCaT cells. Higher concentrations of baicalein generated an increased percentage of cell fraction in the Sub  $G_0$  cell cycle stage, indicating apoptosis. Lower concentrations of baicalein promoted HaCaT proliferation, while higher concentrations induced apoptosis. These results corroborate the findings from an earlier study from our group<sup>25</sup> on the influence of baicalein treatment on L929 fibroblast cells. It was observed that lower concentrations of baicalein (below 10  $\mu\text{M}$ ) were nontoxic to L929 cells and promoted cell proliferation.

#### Lower concentrations of baicalein accelerated *in vitro* wound healing than higher concentrations in HaCaT cells

As the migration of different cell types towards the wound area is a vital step during wound healing, *in vitro* wound healing assays mimicking the proliferative phase of wound healing, are employed to evaluate the wound healing potential of compounds and phytochemicals prior to animal experiments<sup>26</sup>. *In vitro* scratch wound assay widely substitutes animal models for studying wound healing because of its reproducibility, easiness, and cost-effectiveness.

In this study, the *in vitro* scratch wound assay was executed on a confluent monolayer of HaCaT keratinocytes. Images of the wound area, captured at 24 and 48 h after applying baicalein (Fig. 4A), were analysed for cellular migration using ImageJ software. The percentage of wound closure was estimated from the wound gap area evaluated at each time point. It was observed that, in HaCaT cells, wound closure rate was accelerated than control at lower concentrations (5  $\mu\text{M}$ ) and reduced at higher concentrations (50  $\mu\text{M}$ ) by baicalein (Fig. 4B). HaCaT cells are the most suitable and commonly used cell type for the *in vitro* scratch wound assay<sup>15,27</sup>. Hence, the outputs from the

*in vitro* scratch wound assay in the current study substantiate the pro-wound healing activity of lower concentrations of baicalein.

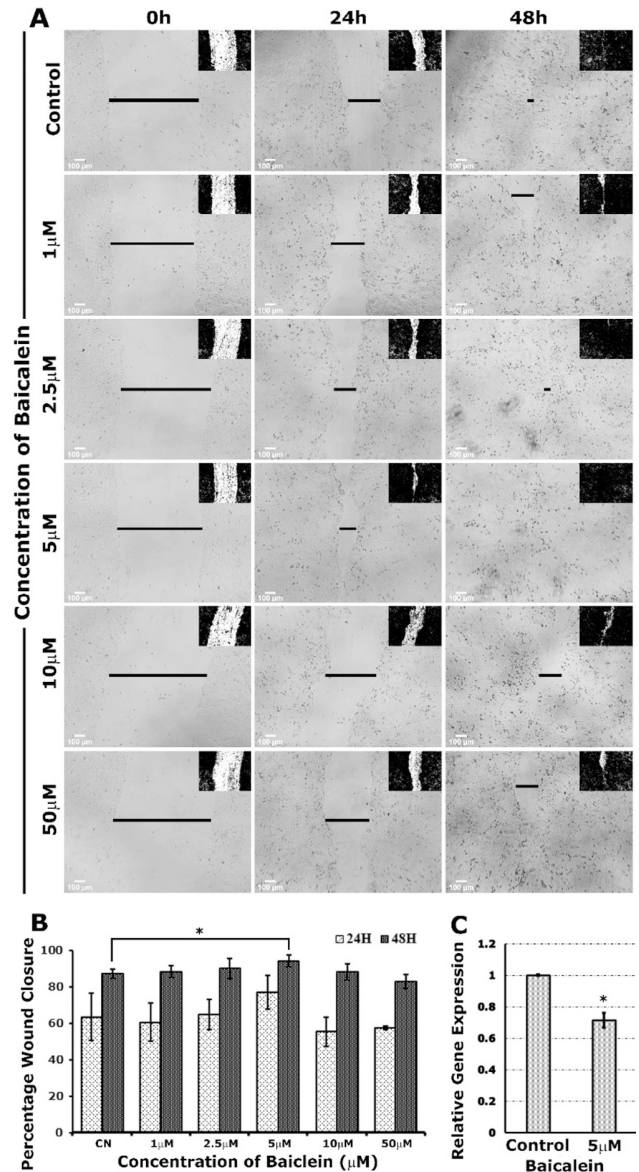


Fig. 4 — *In vitro* scratch wound assay. (A) Representative phase contrast images of the monolayer of HaCaT cells undergoing wound closure after 24 and 48 h of wounding and baicalein treatment. A horizontal straight line spans the residual wound area for each image to indicate the wound closure rate. A representative black-and-white image generated by ImageJ software to indicate the wound area (white colour) is provided as an inset for each sample. (B) ImageJ software calculated the wound area at 0, 24 and 48 h of baicalein treatment and plotted it as a bar graph of the average percentage of wound closure for three experiments. (C) Relative gene expression of Keratin 10 in a monolayer of HaCaT cells after *in vitro* wounding by scratch subsequent treatment with 5  $\mu\text{M}$  of baicalein for 48 h. [\* $P < 0.05$  compared to control]

### Baicalein downregulated the expression of Keratin 10 in HaCaT cells

Keratins are fibrous proteins that provide the structural frameworks of keratinocytes. The expression of different types of keratin proteins characterises the specific subtypes of keratinocytes. Keratin 10 is the primary keratin protein produced by the differentiated keratinocytes present in the outermost layer of the epidermis. Keratin 10 complexes with the Keratin 1 protein, which is also produced by the differentiated keratinocytes, to form the keratin intermediate filaments that offer structural integrity to the skin<sup>28</sup>. Keratins also play important roles during the process of wound healing. One of the first steps in epidermal wound healing is the activation of keratinocytes, described by the morphological and gene expression changes leading to the withdrawal of keratinocytes from a terminally differentiated state<sup>29</sup>. The reepithelialisation phase of wound healing starts with activating keratinocytes at the wound margins and their subsequent migration toward the wound bed. Activation of the differentiated keratinocytes is characterised by cellular hypertrophy, formation of F-actin bundles, retraction of keratin filaments, and the downregulation of keratin 10 expression<sup>24</sup>. Hence, the expression level of keratin 10 after baicalein treatment was investigated at the mRNA level by qPCR.

The results show that there is a significant reduction in the relative gene expression of keratin 10 (Fig. 4C) in keratinocytes (HaCaT) subjected to *in vitro* scratch wound assay and treatment with lower concentrations of baicalein (5  $\mu$ M) for 48 h. Also, considering the increased proliferation observed in HaCaT cells at this concentration of baicalein (Fig. 1), it may be put forward

that baicalein at lower concentrations could augment the pace of reepithelialisation during wound healing. The pattern of the reepithelialisation phase determines the prognosis of a wound-healing event, as it was observed from earlier studies that delayed reepithelialisation resulted in chronic non-healing wounds<sup>30</sup>. Although it may be proposed that baicalein promotes the activation of keratinocytes from the reduced expression level of KRT10 mRNA, the gene expression studies of other markers of activated keratinocytes, namely, KRT6, KRT16 and KRT17, are warranted<sup>24</sup>.

### Improved angiogenesis was observed in CAM treated with lower concentrations of baicalein

Chorioallantoic membrane (CAM) assay is an extensively used model for studying pro-angiogenic and anti-angiogenic properties of biomolecules due to its simplicity, lower cost, resemblance to *in vivo* physiology, and room for improvisation<sup>16</sup>. The current study has also utilised the CAM assay to assess the angiogenic potential of baicalein. The proliferative lower concentrations of baicalein (below 10  $\mu$ M) were used for the experiment. Since the pro-angiogenic potential of baicalein was being investigated, the assay was carried out on fertilised eggs on the fourth day of incubation<sup>31</sup>. The allantoic membrane starts developing in the embryo after 3.5 days of incubation and continues proliferating till 11 days. The CAMs were visually investigated and imaged after 72 h of incubation, as suggested previously for angiogenic assays<sup>32</sup>.

Improved angiogenesis was observed in CAM assay when treated with 2.5, 5 and 10  $\mu$ M of baicalein. CAM subjected to treatment with 2.5  $\mu$ M of baicalein displayed more branching and density of blood vessels (Fig. 5A). The percentage area of blood

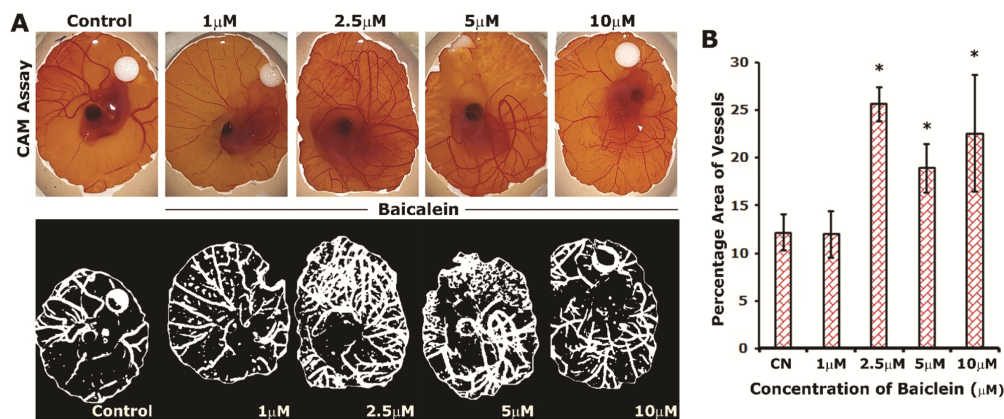


Fig. 5 — CAM assay. (A) Images showing the blood vessels formed on CAM after treatment with the indicated concentrations of baicalein after 72 h. The lower panels are representative binary images developed using ImageJ software while analysing the percentage area of the vasculature on CAM. (B) Graphical representation of the image analysis of the blood vessels of CAM using ImageJ software after treatment with different concentrations of baicalein (n=4). [\*  $P < 0.05$  compared with control]

vessels on CAM calculated using ImageJ software also substantiated the qualitative observations after visual investigation (Fig. 5A). These results are suggestive of the pro-angiogenic effect of lower concentrations of baicalein.

The observations from the *in vitro* and *in ovo* experiments highlight the potential of baicalein as a lead molecule for prospective wound healing applications. There are conflicting reports on the angiogenic effects of baicalein<sup>7,13</sup>. Results from experiments illustrated here emphasize the significance of the effective concentration of baicalein on treatment output. Notably, the proliferative, pro-migratory, and angiogenic activities of baicalein on HaCaT cells were pronounced in lower concentrations (below 10  $\mu$ M). In comparison, higher concentrations of baicalein were pro-apoptotic and exhibited a less significant effect on wound healing. Lower concentrations of baicalein also appear to activate keratinocytes, augmenting the reepithelialisation phase of wound healing. Previous studies from our group showed the potential of baicalein in inducing improved proliferation, migration of fibroblasts, and expression of collagen protein<sup>25</sup>. Moreover, modern wound dressing fabrication strategies try to incorporate angiogenesis-inducing components<sup>33</sup>. Hence, baicalein is worth investigating further for the possible utility in developing upgraded wound dressings to treat non-healing wounds.

One major challenge in the clinical and economic utility of baicalein is its lesser water solubility and bioavailability. Currently, numerous investigations are underway to explore various strategies to improve these physiochemical aspects of baicalein, such as the use of drug-delivery systems based on nanocrystals, nano-micelles, emulsions, solid dispersion, etc., as well as the use of excipients such as cyclodextrin<sup>34</sup>.

#### **Baicalein spontaneously binds to the ERR $\alpha$ -PGC1 $\alpha$ complex *in silico***

To effectively use baicalein as a critical component in wound dressings, it is essential to delineate the molecular pathways by which it promotes angiogenesis. Baicalein is reported to behave as a hypoxia-mimetic<sup>7</sup>, and its physiological response involves the stabilisation of HIF-1<sup>7,10</sup>. HIF-1 transcriptionally regulates the expression of VEGF, the primary molecular facilitator of angiogenesis<sup>3</sup>. Alternatively, VEGF expression is also observed to be regulated by various HIF-independent mechanisms<sup>4,5</sup>. In this study, the authors attempted to evaluate, *in silico*, whether the pro-angiogenic potential of the hypoxia-mimicking agent, baicalein, is effected via a hypoxia-dependent or independent pathway.

The molecular cascade of proteins involved in the hypoxia-dependent regulation of HIF-1 is the most obvious area to be investigated for studying the mode of action of baicalein. HIF1 is a transcription factor with two subunits in its functionally active form: HIF-1 $\beta$ , the constitutively expressed subunit, and HIF-1 $\alpha$ , the oxygen-dependent subunit. The stability of HIF-1 $\alpha$  is controlled by its post-translational modifications, such as hydroxylation and acetylation<sup>35</sup>. The oxygen-dependent regulation of HIF is carried out by prolyl hydroxylase enzyme (PHD) of the 2-oxoglutarate-dependent dioxygenase family. Under normoxic conditions, PHD2 (Prolyl hydroxylase-2) hydroxylates proline residues and acetylates a lysine residue of the oxygen-dependent degradation domain (ODDD) of HIF-1 $\alpha$ . This triggers the association of HIF-1 $\alpha$  with the von Hippel-Lindau (pVHL) E3 ligase complex. VHL, which is a tumour-suppressor protein, is the recognition component of an E3 ubiquitin-protein ligase. VHL binding is also promoted by the acetylation of lysine (K) residue 532 by the ARD1 acetyltransferase, leading to HIF-1 $\alpha$  degradation via the ubiquitin-proteasome pathway. Under hypoxia, the HIF-1 $\alpha$  subunit level is stabilised as it does not undergo degradation. It interacts with coactivators, such as cAMP response element-binding protein (CBP)/p300 and regulates the expression of target genes by binding to the HIF-1-inducible hypoxia-responsive element (HRE) on DNA<sup>35</sup>. Another enzyme regulating HIF-1 $\alpha$  stability is the factor-inhibiting HIF-1 $\alpha$  (FIH-1), which acts via the hydroxylation of asparaginyl residue on HIF-1 $\alpha$ , leading to proteasomal degradation<sup>36</sup>. This post-translational modification also inhibits the binding of HIF-1 $\alpha$  to CBP/p300, thereby reducing the transcriptional potential of HIF-1. Hence, PHD2 is the principal HIF-specific prolyl hydroxylase, while FIH1 is a HIF-specific asparaginyl hydroxylase, destabilising HIF1 $\alpha$  protein levels in normal conditions.

Thus, to carry out the docking studies of baicalein with molecules involved in the HIF-dependent angiogenesis pathway, the proteins chosen are PHD2 and FIH1. At normal conditions, before adding baicalein, both PHD2 and FIH1 exist as complexes with 2-OG (2-oxoglutarate), which is bound to iron (II) at the active site. Therefore, via docking analysis, we investigated whether baicalein can bind to the active site of PHD2 and FIH1 by competitively removing 2-OG.

The 3D structures for molecular docking analysis were secured from the crystallographic structures available in the Protein Data Bank. The 3D structures

of both PHD2 and FIH1 complexed with 2-oxoglutaric acid were identified from the literature as having PDB ID, 3OUJ<sup>37</sup> and 1MZF<sup>38</sup>, respectively. Baicalein (PubChem ID – 5281605) was used as the ligand for both proteins. Since the competitive inhibitory activity of baicalein was being investigated, the site of 2-OG binding was decided as the docking site. Using the Schrödinger software, 2-OG was located in both the protein complexes, extracted and saved as a separate ligand molecule. These respective locations on the protein molecule were designated as the grid positions for the docking analysis (Suppl. Table S2).

Molecular docking with baicalein as well as 2-OG was performed for both proteins at the 2-OG binding pocket. 3OJU could not make any significant interactions with baicalein. 3OUJ-2-OG interaction complex is shown in Suppl Fig. S1. The negative docking score (Table 1) indicated that 1MZF could

spontaneously bind to baicalein (-3.642). But, since a lesser energy score was obtained when docked with 2-OG (-9.034), baicalein seems unable to bind with 1MZF by competitively removing 2-OG. The corresponding docking complexes illustrated as 3D ribbon structures and interaction images are given in Fig. 6 A(i) and Fig 6 A(ii), respectively.

Table 1 — List of docking scores generated for each protein-ligand combination

PDB ID-Ligand Complex	Docking Score
3OUJ-2OG complex	-9.903
3OUJ-Baicalein complex	No Docking
2G1M-2OG complex	-11.731
2G1M-Baicalein complex	-7.682
1MZF-2OG complex	-9.034
1MZF-Baicalein complex	-3.642
1MZE-2OG complex	-8.033
1MZE-Baicalein complex	-5.323
7E2E-Baicalein complex	-9.603

[2OG – 2 Oxoglutaric acid]

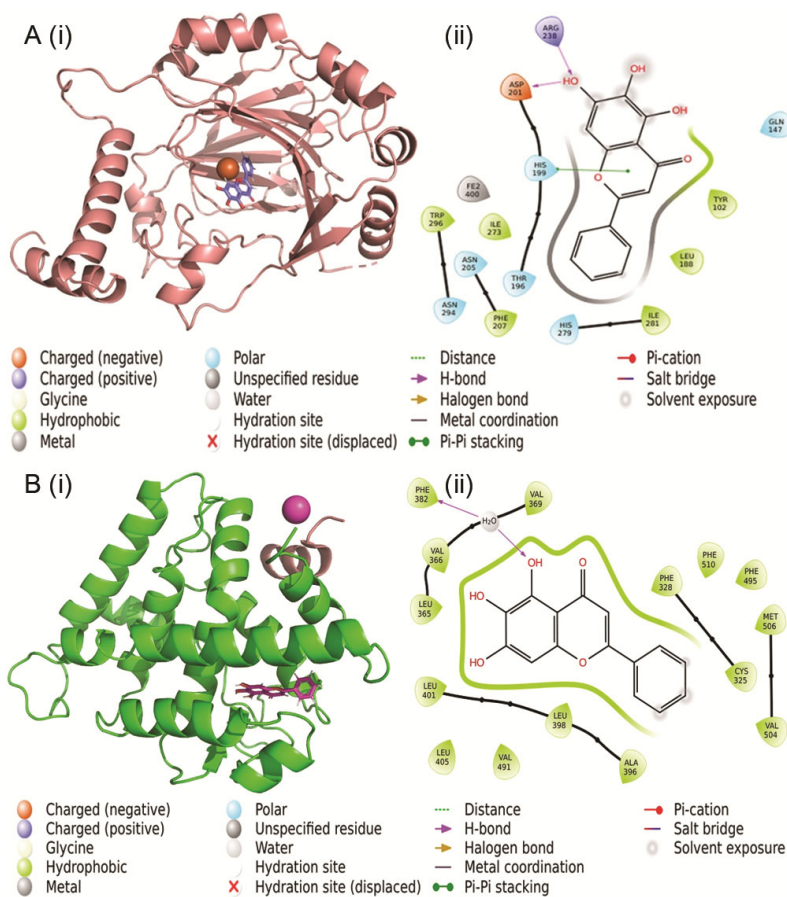


Fig. 6 — Baicalein docked with (A) FIH1 (PDB ID – 1MZF); and (B) ERR $\alpha$ -PGC1 $\alpha$  complex (PDB ID – 7E2E) depicted as a (i) 3D ribbon diagram; and (ii) stick diagram. [The legend in the lower margin of the figure enlists the scheme to specify the types of interactions and molecules involved. Iron is depicted as the small spherical structure in the middle of the protein in 6A. In 6B, the spherical structure bordering the structure is Iodine ion. The darker helix near the Iodine, at the right-top corner, is the 12-mer chain of PGC1 $\alpha$ ]

The results hence indicate that baicalein may not be able to bind with both PHD2 and FIH1 when in native conformation, complexed with 2-OG, inside a cell. The binding pockets used for the docking experiment were optimised for 2-OG, as they are identified in 3D crystallographic structures already bound with 2-OG. This rigid pocket might have hindered the free binding of baicalein with the protein molecules. In order to confirm the results, molecular docking was repeated with PHD2 and FIH1 structures, not in complex with 2-OG. PDB IDs 2G1M (for PHD2)<sup>39</sup> and 1MZE (for FIH1)<sup>38</sup> docked with both baicalein and 2-OG at the ligand binding site. This docking procedure also revealed that even though baicalein spontaneously interacts with both 2G1M (Docking Score: -7.682) and 1MZE (Docking Score: -5.323), it has lower binding potential than 2-OG as indicated by the more negative docking scores (-11.731 and -8.033, respectively) (Table 1 and Suppl. Figs S1 & S2).

Therefore, it can be inferred from the molecular docking experiments of PHD2 and FIH1 that, under normal physiological conditions, within a cell, when these proteins are in complex with 2-OG, baicalein - although a known hypoxia mimetic - is less likely to bind to them by competitively removing 2-OG. Hence, it is less probable that baicalein stabilises HIF-1 $\alpha$  by inhibiting the HIF hydroxylase enzymes PHD2 and FIH1. This supposition parallels earlier reports from Cho *et al.* that the HIF-1-mediated transcriptional activation is not essential for the angiogenic response to baicalein<sup>10</sup>. This group also demonstrated that even in HIF-1 knockdown 3T3-L1 cells, baicalein treatment upregulated VEGF mRNA expression<sup>10</sup>. Another study by Zhang *et al.*, using baicalin, a glucuronide of baicalein, also concluded that the observed increase in VEGF expression is less likely to be mediated via HIF<sup>40</sup>. They observed that treatment with baicalin and *S. baicalensis* extract did not induce significant HIF-1 $\alpha$  production but induced VEGF expression even with a defective HRE region. These observations lead to the deduction that baicalein exerts its effects primarily via the HIF-independent pathway for VEGF induction<sup>4</sup>.

In addition to the hypoxia response element (HRE) for HIF-1 binding, the VEGF promoter also possesses binding regions for other transcription factors, namely ERR (Estrogen-related receptors), CREB, Ap-1, etc.<sup>40</sup>. Estrogen-related receptors (ERRs) are a family of orphan nuclear hormone receptors initially identified based on their homology to the estrogen

receptor ER $\alpha$ . Hence, an alternate method of VEGF induction involves other transcriptional activation pathways, such as the peroxisome proliferator-activated receptor-coactivator-1 (PGC-1 $\alpha$ ) pathway<sup>5</sup>. PGC-1 $\alpha$  is a coactivator that interacts with ERR $\alpha$  (independent of ligand binding to ERR $\alpha$ ), functionally activates ERR  $\alpha$ , and induces expression of target genes. PGC-1 $\alpha$  co-activates the ERR $\alpha$  bound to specific conserved sites present in the regulatory regions of the VEGF gene. PGC-1 $\alpha$  is known to induce VEGF expression and angiogenesis *in vitro*, in breast cancer cells and muscle cells, and *in vivo*, in skeletal muscle, by activating ERR $\alpha$  in a HIF-1 $\alpha$ -independent manner<sup>40</sup>.

It is generally considered that ERRs are constitutively active and interact with coactivators in the absence of exogenous ligands<sup>40</sup>. ERR $\alpha$  is constitutively active because its ligand binding pocket (LBP) is practically filled with side chains, particularly of Phe-328. Suetsugi *et al.*<sup>41</sup> has shown that several isoflavones (e.g., genistein, daidzein) and a flavone aglycone (6,3',4'-trihydroxyflavone) can bind agonistically to ERR and further increase ERR activity<sup>41</sup>. Baicalein, being a flavone, may attach to ERR $\alpha$  to increase its activity and subsequent VEGF expression. Moreover, former investigators have claimed that baicalin (a glucuronide of baicalein) triggered VEGF production through the ERR $\alpha$ -PGC1 $\alpha$  pathway<sup>40</sup> via the overexpression ERR $\alpha$ . They, however, have also proposed that an alternative mechanism other than overexpression of ERR $\alpha$  may be operating for VEGF induction by baicalein.

Hence, we investigated, via docking analysis, whether baicalein is capable of binding with ERR $\alpha$  complexed with PGC-1 $\alpha$  in an agonistic way, thereby increasing the ERR $\alpha$  activity. We expected baicalein to bind ERR $\alpha$  such that it would not disrupt ERR $\alpha$ -PGC-1 $\alpha$  interaction. The structure of the ERR $\alpha$ -PGC1 $\alpha$  complex attached with an agonist (DS45500853) was utilised for studying this (PDB ID - 7E2E)<sup>42</sup>. Works on the X-ray crystal structure of ERR $\alpha$  ligand-binding domain in complex with agonists and PGC-1 $\alpha$  coactivator peptide have revealed conformational changes in the ligand-binding pocket to accommodate the agonists<sup>43</sup>.

Molecular docking of 7E2E with baicalein was executed at the agonist binding pocket. The docking score obtained was high (-9.603), indicating the ability of 7E2E to bind to baicalein spontaneously (Table 1). The 3D ribbon structures [Fig. 6B(i)] and

the image of the best-docked position, depicting the moieties involved [Fig. 6B(ii)], are given. The interaction image reveals that hydrophobic interactions are primarily involved in the interaction of the protein with baicalein. Similar to how the phenolic hydroxyl group of the agonist, DS45500853, engages in a hydrogen bond (H-bond) with the oxygen atom of Phe-382 of ERR $\alpha$  LBP (ligand binding pocket) via a water molecule<sup>43</sup>, baicalein also forms an H-bond with Phe-382 through a water molecule [Fig 6B(ii)]. When DS45500853 bind to the LBP, the C $\alpha$  atoms of Leu-324, Cys-325, and Phe-328 move to accommodate the ligand, while conformational changes occur for side-chain atoms in Phe-328, Leu-365, Phe-382, and Phe-495<sup>43</sup>. The same amino acids (Cys-325, Leu-365, Phe-495, and Phe-328) are also involved among the moieties interacting with baicalein via hydrophobic forces. Other key hydrophobic interactions are contributed by Val-369, Val-366, Leu-401, Leu-405, Val-491, Leu-398, Ala-396, Val-504, Met-506, and Phe-510 [Fig 6B(ii)].

The outcomes of the *in silico* docking analysis suggest that baicalein can spontaneously bind at the agonistic site of the ERR $\alpha$ -PGC1 $\alpha$  complex, promoting the downstream activation of target genes, including VEGF. This observation validates the claims by former investigators that baicalein induced VEGF expression by promoting the ERR $\alpha$ -PGC1 $\alpha$  activity<sup>40</sup>. These results have to be warranted using knockdown *in vitro* models and further in-depth proteomic and genomic investigations, which are within the future considerations of this work. It was proposed by Shinozuka *et al.* that DS45500853 maintains ERR $\alpha$  by preventing the binding of its endogenous corepressor, RIP140 (receptor-interacting protein 140)<sup>43</sup>. RIP140 is a transcriptional regulator, first identified in estrogen receptor  $\alpha$  (ER $\alpha$ )<sup>44</sup> and later recognised to cooperate with a host of transcription factors, including nuclear receptors<sup>45</sup>. Prior literature has reported that RIP140 inhibits the transactivation of ERR $\alpha$ , ERR $\beta$ , and ERR $\gamma$ <sup>46</sup>. It may be hypothesized that similar to DS45500853, baicalein could also activate ERR $\alpha$  by preventing the binding of RIP140. Hence, it may be concluded from the study that baicalein causes its pro-angiogenic properties mainly through the HIF-independent regulation of VEGF expression.

The economic and social impact of wound care management is immense as it has global markets. This study points out that baicalein is a potential lead

molecule for developing marketable therapeutics for cutaneous wound healing. Data obtained from this study shows that baicalein promotes pro-angiogenesis and wound healing effects at low concentrations in the micromolar range. This fact considerably cuts the quantity of baicalein required, bringing down the product cost. Moreover, Baicalein can be extracted and purified from indigenous plant varieties such as Thumba (*Leucas aspera*)<sup>47</sup> and Indian Trumpet tree (*Oroxylum indicum*)<sup>8</sup>, substantially lowering expenses.

Furthermore, baicalein can be conjugated with efficient drug-delivery systems, which would facilitate sustained release over time. Such systems incorporated into biodegradable wound dressings would decrease the frequency with which dressings would need to be changed, thereby reducing the number of hospital visits, decreasing waste, and significantly lessening the overall costs. This outcome would, in particular, greatly benefit the pediatric and geriatric patient population. These systems can also be coupled with other antimicrobial agents for improved wound healing, another area of interest on which our group works<sup>48</sup>.

## Conclusion

Data obtained from this study show that lower concentrations of baicalein promoted the proliferation and migration of HaCaT keratinocytes and achieved accelerated wound closure *in vitro*. Low concentrations of baicalein also exhibited pro-angiogenic activity, as observed from improved branching and density of blood vessels on the CAM surface. Higher concentrations of baicalein, however, increased the percentage of cell fraction in the Sub G<sub>0</sub> phase of the cell cycle, indicating apoptosis, and had only negligible influence on wound healing *in vitro*. Lower concentrations of baicalein downregulated the expression of keratin 10, suggestive of the subsequent activation of keratinocytes and enhancement of the reepithelialisation phase of wound healing. These results highlight the significance of monitoring and defining accurate, effective concentrations of baicalein during treatment. The observations from both *in vitro* and *in ovo* experiments also advocate the prospects of using baicalein in developing green wound dressings and bioengineered constructs that promote angiogenesis. The study has also adopted *in silico* techniques to understand the underlying mechanisms by which baicalein promotes VEGF expression and angiogenesis. Although baicalein is known to stabilize HIF1 $\alpha$ , the data obtained from *in silico* studies demonstrate that baicalein may not be

efficient in inhibiting PHD2 and FIH1 by competitively replacing 2-OG bound to these proteins in the normoxic native state. Baicalein can, however, efficiently bind with the ERR $\alpha$ -PGC1 $\alpha$  complex at the agonistic binding pocket chiefly through hydrophobic interactions. ERR $\alpha$  is known to promote VEGF expression and enhance angiogenesis. It can be concluded that the pro-angiogenic potential of baicalein can be achieved by the HIF-independent agonistic activation of the ERR $\alpha$ -PGC1 $\alpha$  complex to transcriptionally initiate VEGF expression. Further investigations also need to be carried out on the effects of baicalein in chronic non-healing wounds, where the disease microenvironment and physiological milieu are diverse and require varied wound management strategies.

### Ethical approval

The *in ovo* experiments were excluded from the ethical approval requisite as the experiments were terminated on day 8, within the first half of the gestation period (10 days), for which ethics approval is not mandatory. All other experiments were performed on cell lines.

### Acknowledgement

We acknowledge the financial support from the Kerala State Plan Grant from the University of Kerala for “Strengthening of centers/ interuniversity centers” (UOK NO: 1747/2021/UOK). We thank Dr Annie Abraham (UGC-BRS Emeritus Fellow) and Dr S Gayathri, Department of Biochemistry, University of Kerala, for providing the primer; Dr P Sreejith, Department of Zoology, University of Kerala, for gifting the HaCaT cells; and Dr KC Sivakumar, Bioinformatics Facility and Ms SV Surabhi, FACS Facility, Rajiv Gandhi Centre for Biotechnology for assisting in experiments.

### Conflict of Interest

Authors declare no competing interests.

### Reference

- Nguyen D, Orgill D & Murphy G, The pathophysiologic basis for wound healing and cutaneous regeneration. In: *Biomaterials for Treating Skin Loss*, (Ed. Orgill D & Blanco C; Woodhead Publishing, Cambridge, England), 2009, 25.
- Fong GH, Mechanisms of adaptive angiogenesis to tissue hypoxia. *Angiogenesis*, 11 (2008) 121.
- Zimna A & Kurpisz M, Hypoxia-inducible factor-1 in physiological and pathophysiological angiogenesis: applications and therapies. *BioMed Res Int*, 2015 (2015) 1.
- Mizukami Y, Li J, Zhang X, Zimmer MA, Iliopoulos O & Chung DC, Hypoxia-inducible factor-1-independent regulation of vascular endothelial growth factor by hypoxia in colon cancer. *Cancer Res*, 64 (2004) 1765.
- Arany Z, Foo S-Y, Ma Y, Ruas JL, Bommi-Reddy A, Gimun G, Cooper M, Laznik D, Chinsomboon J, Rangwala SM, Baek KH, Rosenzweig A & Spiegelman BM, HIF-independent regulation of VEGF and angiogenesis by the transcriptional coactivator PGC-1 $\alpha$ . *Nature*, 451 (2008) 1008.
- Stiers P-J, van Gestel N & Carmeliet G, Targeting the hypoxic response in bone tissue engineering: A balance between supply and consumption to improve bone regeneration. *Mol Cell Endocrinol*, 432 (2016) 96.
- Abu-Shahba AG, Gebraad A, Kaur S, Paananen RO, Peltoniemi H, Seppänen-Kajansinkko R & Mannerström B, Proangiogenic Hypoxia-Mimicking Agents Attenuate Osteogenic Potential of Adipose Stem/Stromal Cells. *Tissue Eng Regen Med*, 17 (2020) 477.
- Nik Salleh NNH, Othman FA, Kamarudin NA & Tan SC, The Biological Activities and Therapeutic Potentials of Baicalein Extracted from *Oroxylum indicum*: A Systematic Review. *Molecules*, 25 (2020) 5677.
- Rahmani AH, Almatroudi A, Khan AA, Babiker AY, Alanezi M & Allemailem KS, The multifaceted role of baicalein in cancer management through modulation of cell signalling pathways. *Molecules*, 27 (2022) 8023.
- Cho H, Lee H-Y, Ahn D-R, Kim SY, Kim S, Lee KB, Lee YM, Park H & Yang EG, Baicalein induces functional hypoxia-inducible factor-1 $\alpha$  and angiogenesis. *Mol Pharmacol*, 74 (2008) 70.
- Lee S-I, Kim S-Y, Park K-R & Kim E-C, Baicalein promotes angiogenesis and odontoblastic differentiation via the BMP and Wnt pathways in human dental pulp cells. *Am J Chin Med*, 44 (2016) 1457.
- Lin R, Lin J, Li S, Ding J, Wu H, Xiang G, Li S, Huang Y, Lin D & Gao W, Effects of the traditional Chinese medicine baicalein on the viability of random pattern skin flaps in rats. *Drug Des Devel Ther*, 12 (2018) 2267.
- Liu JJ, Huang TS, Cheng WF & Lu FJ, Baicalein and baicalin are potent inhibitors of angiogenesis: Inhibition of endothelial cell proliferation, migration and differentiation. *Int J Cancer*, 106 (2003) 559.
- Huang Y, Miao Z, Hu Y, Yuan Y, Zhou Y, Wei L, Zhao K, Guo Q & Lu N, Baicalein reduces angiogenesis in the inflammatory microenvironment via inhibiting the expression of AP-1. *Oncotarget*, 8 (2017) 883.
- Brandi J, Cheri S, Manfredi M, Di Carlo C, Vita Vanella V, Federici F, Bombiero E, Bazaj A, Rizzi E, Manna L, Cornaglia G, Marini U, Valenti MT, Marengo E & Cecconi D, Exploring the wound healing, anti-inflammatory, anti-pathogenic and proteomic effects of lactic acid bacteria on keratinocytes. *Sci Rep*, 10 (2020) 11572.
- West DC, Thompson WD, Sells PG & Burbridge MF, Angiogenesis Assays Using Chick Chorioallantoic Membrane. In: *Angiogenesis Protocols*, (Ed. Murray JC; Humana Press, Totowa, NJ), 2001, 107.
- Lei X, Liu B, Han W, Ming M & He Y-Y, UVB-Induced p21 degradation promotes apoptosis of human keratinocytes. *Photochem Photobiol Sci*, 9 (2010) 1640.
- Haron AS, Syed Alwi SS, Saiful Yazan L, Abd Razak R, Ong YS, Zakarial Ansar FH & Roshini Alexander H, Cytotoxic effect of thymoquinone-loaded nanostructured lipid carrier (TQ-NLC) on liver cancer cell integrated with

- hepatitis B genome, Hep3B. *Evid Based Complement Alternat Med*, 2018 (2018) 1.
- 19 El Darzi E, Bazzi S, Daoud S, Echtay KS & Bahr GM, Differential regulation of surface receptor expression, proliferation, and apoptosis in HaCaT cells stimulated with interferon- $\gamma$ , interleukin-4, tumor necrosis factor- $\alpha$ , or muramyl dipeptide. *Int J Immunopathol Pharmacol*, 30 (2017) 130.
  - 20 Galgon T, Wohlrab W & Dräger B, Betulinic acid induces apoptosis in skin cancer cells and differentiation in normal human keratinocytes. *Exp Dermatol*, 14 (2005) 736.
  - 21 Kawano Y, Patrulea V, Sublet E, Borchard G, Iyoda T, Kageyama R, Morita A, Seino S, Yoshida H & Jordan O, Wound healing promotion by hyaluronic acid: Effect of molecular weight on gene expression and in vivo wound closure. *Pharmaceuticals*, 14 (2021) 301.
  - 22 Suh YK, Robinson A, Zanghi N, Kratz A, Gustetic A, Crow MM, Ritts T, Hankey W & Segarra VA, Introducing Wound Healing Assays in the Undergraduate Biology Laboratory Using Ibidi Plates. *J Microbiol Biol Educ*, 23 (2022) e00061.
  - 23 Paddock HN, Schultz GS & Mast BA, Methods in Reepithelialization. A Porcine Model of Partial-Thickness Wounds. In: *Wound Healing: Methods and Protocols*, (Ed. DiPietro LA & Burns AL; Humana Press, Totowa, NJ), 2003, 17.
  - 24 Patel GK, Wilson CH, Harding KG, Finlay AY & Bowden PE, Numerous keratinocyte subtypes involved in wound re-epithelialization. *J Invest Dermatol*, 126 (2006) 497.
  - 25 Mathew KA, Madathil BK, John A & Antony H, Evaluation of baicalein in wound healing: an *in vitro* study. In: *Proceedings of International Conference on Recent Advances in Biological Science*, (Ed. Beevy SS, Menon DB, Saranya MK, Anil Kumar TR & Cherian M; iCEIB, University of Kerala, Thiruvananthapuram, Kerala, India), 2023, 75.
  - 26 Martinotti S & Ranzato E, Scratch Wound Healing Assay. *Methods Mol Biol*, 2109 (2020) 225.
  - 27 Seo E, Lim JS, Jun J-B, Choi W, Hong I-S & Jun H-S, Exendin-4 in combination with adipose-derived stem cells promotes angiogenesis and improves diabetic wound healing. *J Transl Med*, 15 (2017) 1.
  - 28 Roth W, Kumar V, Beer HD, Richter M, Wohlenberg C, Reuter U, Thiering S, Staratschek-Jox A, Hofmann A, Kreuzsch F, Schultze JL, Vogl T, Roth J, Reichelt J, Hausser I & Magin TM, Keratin 1 maintains skin integrity and participates in an inflammatory network in skin through interleukin-18. *J Cell Sci*, 125 (2012) 5269.
  - 29 Grinnell F, Wound repair, keratinocyte activation and integrin modulation. *J Cell Sci*, 101 (1992) 1.
  - 30 Larjava H, Koivisto L & Häkkinen L, Keratinocyte interactions with fibronectin during wound healing. In: *Madame Curie Bioscience Database [Internet]*, (Landes Bioscience), 2013.
  - 31 Sudhakar M, Silambanan S, Prabhakaran AA & Ramakrishnan R, Angiogenic Potential, Circulating Angiogenic Factors and Insulin Resistance in Subjects with Obesity. *Indian J Clin Biochem*, 36 (2021) 43.
  - 32 Ribatti D, The chick embryo chorioallantoic membrane (CAM). A multifaceted experimental model. *Mech Dev*, 141 (2016) 70.
  - 33 Ahmad N, *In Vitro* and *In Vivo* Characterization Methods for Evaluation of Modern Wound Dressings. *Pharmaceutics*, 15 (2022) 42.
  - 34 Mo F, Ma J, Zhang P, Zhang D, Fan H, Yang X, Zhi L & Zhang J, Solubility and thermodynamic properties of baicalein in water and ethanol mixtures from 283.15 to 328.15 K. *Chem Eng Commun*, 208 (2021) 183.
  - 35 Lee JW, Bae SH, Jeong JW, Kim SH & Kim KW, Hypoxia-inducible factor (HIF-1)alpha: its protein stability and biological functions. *Exp Mol Med*, 36 (2004) 1.
  - 36 Mahon PC, Hirota K & Semenza GL, FIH-1: a novel protein that interacts with HIF-1 $\alpha$  and VHL to mediate repression of HIF-1 transcriptional activity. *Genes Dev*, 15 (2001) 2675.
  - 37 Rosen MD, Venkatesan H, Peltier HM, Bembenek SD, Kanelakis KC, Zhao LX, Leonard BE, Hocutt FM, Wu X & Palomino HL, Benzimidazole-2-pyrazole HIF prolyl 4-hydroxylase inhibitors as oral erythropoietin secretagogues. *ACS Med Chem Lett*, 1 (2010) 526.
  - 38 Dann III CE, Bruick RK & Deisenhofer J, Structure of factor-inhibiting hypoxia-inducible factor 1: An asparaginyl hydroxylase involved in the hypoxic response pathway. *Proc Nat Acad Sci*, 99 (2002) 15351.
  - 39 McDonough MA, Li V, Flashman E, Chowdhury R, Mohr C, Liénard BM, Zondlo J, Oldham NJ, Clifton IJ & Lewis J, Cellular oxygen sensing: Crystal structure of hypoxia-inducible factor prolyl hydroxylase (PHD2). *Proc Nat Acad Sci*, 103 (2006) 9814.
  - 40 Zhang K, Lu J, Mori T, Smith-Powell L, Synold TW, Chen S & Wen W, Baicalin increases VEGF expression and angiogenesis by activating the ERR $\alpha$ /PGC-1 $\alpha$  pathway. *Cardiovasc Res*, 89 (2011) 426.
  - 41 Suetsugi M, Su L, Karlsberg K, Yuan Y-C & Chen S, Flavone and Isoflavone Phytoestrogens Are Agonists of Estrogen-Related Receptors1. *Mol Cancer Res*, 1 (2003) 981.
  - 42 Kallen J, Lattmann R, Beerli R, Blechschmidt A, Blommers MJ, Geiser M, Ottl J, Schlaeppi J-M, Strauss A & Fournier B, Crystal structure of human estrogen-related receptor  $\alpha$  in complex with a synthetic inverse agonist reveals its novel molecular mechanism. *J Biol Chem*, 282 (2007) 23231.
  - 43 Shinozuka T, Ito S, Kimura T, Izumi M & Wakabayashi K, Discovery of a Novel Class of ERR $\alpha$  Agonists. *ACS Med Chem Lett*, 12 (2021) 817.
  - 44 Cavailles V, Dauvois S, L'Horset F, Lopez G, Hoare S, Kushner PJ & Parker M, Nuclear factor RIP140 modulates transcriptional activation by the estrogen receptor. *EMBO J*, 14 (1995) 3741.
  - 45 Ho PC & Wei LN, Biological activities of receptor-interacting protein 140 in adipocytes and metabolic diseases. *Curr Diabetes Rev*, 8 (2012) 452.
  - 46 Castet A, Herledan A, Bonnet S, Jalaguier S, Vanacker JM & Cavailles V, Receptor-interacting protein 140 differentially regulates estrogen receptor-related receptor transactivation depending on target genes. *J Mol Endocrinol*, 20 (2006) 1035.
  - 47 Das SN, Patro VJ & Dinda SC, A review: Ethnobotanical survey of genus *Leucas*. *Pharmacogn Rev*, 6 (2012) 100.
  - 48 Mathew KA, Madathil BK & Antony H, Hypoxia mimetics and silver nitrate combination with potential application in wound healing. In: *Book of Abstracts - International Conference on Emerging Trends in Genomics and Biomedicine*, (IUCGGT, University of Kerala, Thiruvananthapuram, Kerala, India), 2023, 42.